

Simple de-embedding and simulation technique to find permittivity with a THz vector network analyser

Jonathan Hammler, Andrew J. Gallant, and Claudio Balocco

School of Engineering and Computing Sciences, Durham University, South Road, Durham, DH1 3LE, United Kingdom

Abstract—A simple and fast method for measuring the dielectric constant with a THz vector network analyser (VNA) has been developed. A numeric de-embedding technique removes free-space propagation effects, then simulation of Maxwell’s equations simultaneously fits both permittivity and thickness to measured scattering parameters. Results are presented for semiconductor and dielectric samples within the frequency range 750 GHz to 1.1 THz, showing excellent agreement with prior work. A statistical analysis of uncertainty is performed, which demonstrates the robustness of our method.

I. INTRODUCTION

WHILE dielectric properties of many materials have been extensively characterised at low frequencies and into the microwave region of the electromagnetic spectrum, published information is much sparser in the THz region. Knowledge of permittivity is essential for design, realisation and commercialisation of devices operating in the so-called terahertz gap. A system based around a THz vector network analyser (VNA) was assembled to measure the scattering parameters of planar samples in the frequency domain. The number of components required is vastly smaller than that of time domain spectroscopy systems, reducing system complexity.

Free-space propagation of the reference and measured electric fields enabled measurements to be taken without contacting the sample. Non-destructive testing of samples is possible since no machining to fit within a resonant cavity or waveguide is required. The methodology results in a simpler, expedited measurement process.

II. METHODOLOGY

The measurement system consists of just two horn antennas fed by VNA frequency extension transceivers, two parabolic mirrors, and a sample holder located in the middle of the collimated beam. This arrangement is shown in Fig. 1. THz frequency transceivers contain Schottky diode multipliers and sub-harmonic mixers, which are used to convert a Keysight N5224A four port VNA operating between 10 MHz – 43.5 GHz to a two port analyser working at 0.75 THz – 1.1 THz. Calibration standards have been used to perform a SOLT (Short, Open, Load, Through) calibration at the waveguide flanges used to mount horn antennas.

Scattering parameters, measured in the absence of a sample, were used to computationally move the measurement plane to the surface of the samples to be characterised. Equations (1) – (3) mathematically describe the process. The system is modelled as three stratified regions of differing permittivity in

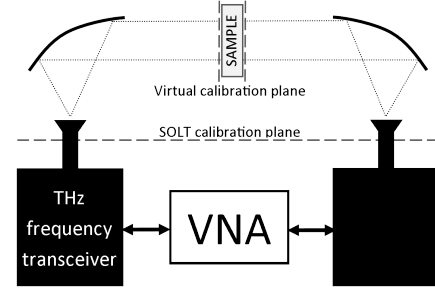


Fig. 1. Schematic representation of the measurement system. Two 90° off-axis parabolic mirrors direct a collimated THz beam through a planar sample.

series; the sample or a slab of air (\mathbf{T}_{air}) flanked by \mathbf{T}_E , free-space propagation regions either side of the sample holder.

$$\mathbf{T}_{measured} = \mathbf{T}_E \cdot \mathbf{T}_{DUT} \cdot \mathbf{T}_E \quad (1)$$

$$\mathbf{A} = \mathbf{T}_{air}^{-1} \cdot \sqrt{\mathbf{T}_{air} \cdot \mathbf{T}_{empty}} \quad (2)$$

$$\mathbf{T}_{DUT} = \mathbf{A}^{-1} \cdot \mathbf{T}_{measured} \cdot \mathbf{A}^{-1} \quad (3)$$

\mathbf{T}_{empty} represents the S-parameter response of the system without a sample in place, converted to ABCD-parameters for ease of calculation. $\mathbf{T}_{measured}$ contains the S-parameter measurements taken with a sample in place. Equation (3) expresses the effect of sample insertion, normalised against the measurement system with the sample absent assuming \mathbf{T}_E is constant between measurement sweeps.

Recording a set of S-parameter measurements is significantly faster than performing a TRL (Through, Reflect, Line) calibration, allowing for samples of differing thicknesses to be quickly and accurately characterised without performing additional precision measurement and recalibration steps. The de-embedding matrix transformation can be adapted to eliminate the effects of different mounting jigs by accounting for their interaction with the probing beam.

Our iterative method simultaneously determines sample thickness and relative permittivity through numerical simulation of Maxwell’s equations, which enforce continuity of electric and magnetic field vectors at material interfaces. Magnitude and phase of both field vectors are calculated by summing forward and reverse travelling waves, modelled as exponential functions $E(z) = E_0 e^{-jkz}$ with a propagation constant $k = \frac{2\pi\sqrt{\epsilon_r}}{\lambda_0}$. The sum of forward and reverse travelling waves with an incident wave magnitude equal to one results in calculating S-parameters. A constrained nonlinear optimisation process was employed to minimise the difference between

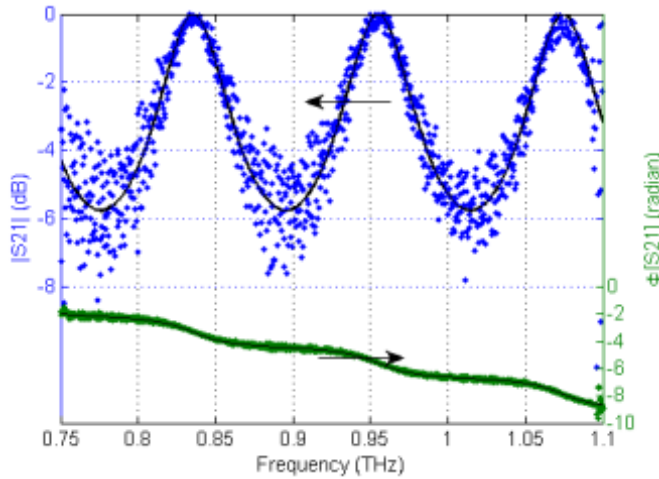


Fig. 2. Magnitude and unwrapped phase of GaAs wafer forward transmission. Solid lines show simulated data, $d = 348\mu\text{m}$, $\epsilon_r = 13.01$, fitted to measured data with $R^2 = 0.981$.

measured transmission and reflection data with simulated data by varying the permittivity and thickness parameters when simulating S-parameters.

III. RESULTS

Both dielectric and semiconductor samples were characterised with our method. Figure 2 shows a typical example of the results obtained for a gallium arsenide wafer. Extrapolated thickness values were verified against measurements taken with a micrometer and were found to be in excellent agreement. Likewise, calculated permittivity values are in agreement with both published material data, where available, and alternative algorithms as shown in Table I.

TABLE I
COMPARISON OF PERMITTIVITY VALUES EXTRACTED WITH TWO DIFFERENT INVERSION TECHNIQUES.

Material	Iterative Method	Non-Iterative [1]	Difference
Si	11.19	11.93	6.60%
GaAs	12.85	12.75	-0.70%
Polystyrene	2.45	2.544	3.80%
HR-Si	11.57	11.27	-2.60%

An uncertainty analysis was performed using statistical methods to characterise the robustness of the system. A principal component analysis was performed on thousands of S-parameter measurements to quantify the variance and distribution of random measurement errors, presented in Fig. 3. This information was used with variances of measured sample thicknesses to perturb the fitting algorithm in Monte Carlo simulations. Accurate dielectric characterisation is performed despite limited accuracy and precision of thickness information; standard deviation of the output quantities was found to be three orders of magnitude smaller when compared to the output from a non-iterative algorithm. This finding indicates that the presented methodology is vastly more resilient to measurement errors. Figure 4 shows the combinations of

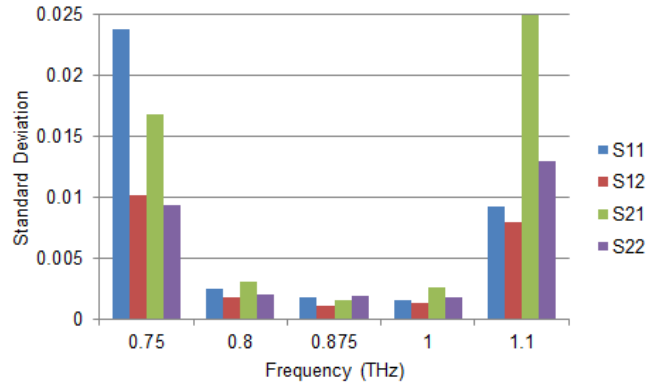


Fig. 3. Magnitude of standard deviations of measured S-parameters indicates measurement uncertainty is highest as the upper and lower operating frequencies are approached.

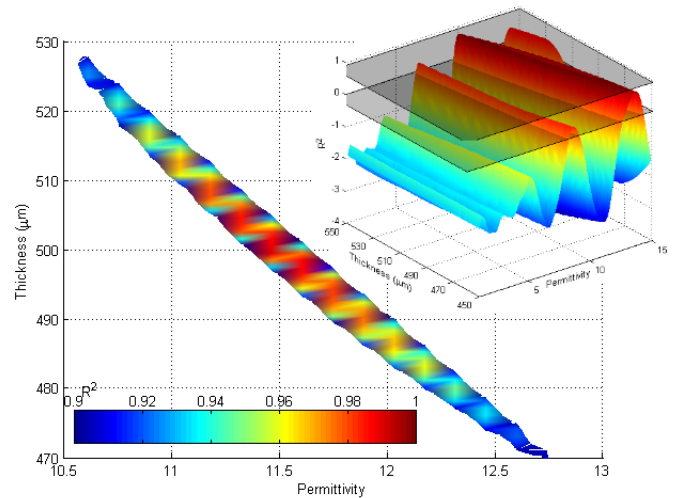


Fig. 4. R^2 (the coefficient of determination) quantifies how well simulated S-parameters, resulting from combinations of relative permittivity and thickness, match measured data from a GaAs wafer.

Inset: Entire search space of the fitting algorithm. Planes cut the surface, delimiting unfeasible solutions $R^2 \leq 0$ and likely solutions $R^2 > 0.9$.

permittivity and thickness simulated during Monte Carlo simulation and their resulting fitness value.

IV. SUMMARY

A new approach to characterising materials in the frequency domain simplifies both equipment setup and the measurement process. The time required to perform a measurement is greatly reduced, at the expense of longer computation times. This system topology would be well suited for process control requiring high sample throughput where sample thickness can be approximated by a population average.

REFERENCES

- [1] A. Kazemipour, M. Hudlicka, T. Kleine-Ostmann, and T. Schrader, "A reliable simple method to extract the intrinsic material properties in millimeter/sub-millimeter wave domain," in *Proc. Conf. Precision Electromagnetic Measurements*, Rio de Janeiro, BR, Aug. 2014, pp. 576–577.